VERSITA

CELLULAR & MOLECULAR BIOLOGY LETTERS
http://www.cmbl.org.pl

Received: 15 November 2012
Final form accepted: 13 April 2013
Published online: April 2013

Volume 18 (2013) pp 249-262
DOI: 10.2478/s11658-013-0087-y

Research article

U937 VARIANT CELLS AS A MODEL OF APOPTOSIS WITHOUT CELL DISINTEGRATION

GRZEGORZ STASIŁOJĆ[1], SANDRA PINTO[3], ROKSANA WYSZKOWSKA[1], MAGDA WEJDA[1,4], EWA M. SŁOMIŃSKA[2], MARTYNA FILIPSKA[1], PATRYCJA KOSZAŁKA[1], JULIAN ŚWIERCZYŃSKI[2], JOSE ENRIQUE O'CONNOR[3] and JACEK JERZY BIGDA[1]*

[1]Department of Cell Biology, Intercollegiate Faculty of Biotechnology UG-MUG, Medical University of Gdansk, Poland, [2]Department of Biochemistry, Faculty of Medicine, Medical University of Gdansk, Poland, [3]Cytomics Laboratory, Mixed Unit University of Valencia - Prince Felipe Research Center, Valencia, Spain, [4]Department for Molecular Biomedical Research, Flanders Institute for Biotechnology and the Department of Biomedical Molecular Biology, Ghent University, Ghent, Belgium (current address)

Abstract: The variant cell line $U937_V$ was originally identified by a higher sensitivity to the cytocidal action of tumor necrosis factor alpha (TNFα) than that of its reference cell line, U937. We noticed that a typical morphological feature of dying $U937_V$ cells was the lack of cellular disintegration, which contrasts to the formation of apoptotic bodies seen with dying U937 cells. We found that both TNFα, which induces the extrinsic apoptotic pathway, and etoposide (VP-16), which induces the intrinsic apoptotic pathway, stimulated $U937_V$ cell death without cell disintegration. In spite of the distinct morphological differences between the U937 and $U937_V$ cells, the basic molecular events of apoptosis, such as internucleosomal DNA degradation, phosphatidylserine exposure on the outer leaflet of the plasma membrane, caspase activation and cytochrome c release, were evident in both cell types

* Author for correspondence: Department of Cell Biology, Medical University of Gdańsk, ul. Dębinki 1, 80-211 Gdańsk, Poland. Tel. +48 58 3491434; fax. +48 58 3491445; jjbigd@gumed.edu.pl

Abbreviations used: ATCC – American Type Culture Collection; CHX – cycloheximide; DCF – 2,7-dichlorofluorescin; DHCF-DA – 2',7'-dihydrodichlorofluorescein diacetate; DHE – dihydroethidium; MMP – mitochondrial membrane potential; $^{\cdot}O_2^-$ – superoxide anion; PS – phosphatidylserine; TMRM – tramethylrhodamine methyl ester; TNFα – tumor necrosis factor; $U937_V$ – a variant of the U937 cell line; VP-16 – etoposide

when stimulated with both types of apoptosis inducer. In the $U937_V$ cells, we noted an accelerated release of cytochrome c, an accelerated decrease in mitochondrial membrane potential, and a more pronounced generation of reactive oxygen species compared to the reference cells. We propose that the U937 and $U937_V$ cell lines could serve as excellent comparison models for studies on the mechanisms regulating the processes of cellular disintegration during apoptosis, such as blebbing (zeiosis) and apoptotic body formation.

Key words: Apoptosis, U937 cells, Apoptotic bodies, Cell disintegration

INTRODUCTION

Apoptosis is one of the most studied mechanisms of cell death. Apoptotic cells are characterized by cytoplasmic and organelle contraction and shrinkage and nuclear chromatin condensation [1]. In the terminal stages, cell membranes undergo blebbing (zeiosis) [2] and then the cells disintegrate into apoptotic bodies [1, 3, 4]. Among the biochemical markers of apoptosis are exposure of phosphatidylserine (PS) on the outer leaflet of the cell membrane, a decrease in mitochondrial membrane potential, release of cytochrome c from the mitochondria, activation of caspases and internucleosomal fragmentation of DNA [5].

There are two interdependent pathways of apoptosis initiation. The extrinsic pathway is mediated by the death receptors, such as CD95 and TNFRs, and the intrinsic pathway is mediated by the mitochondria and endoplasmic reticulum [6, 7]. An important event of the extrinsic pathway is the activation of caspase-8, which triggers not only the executioner caspases like caspase-3 and caspase-6, but can also result in the activation of the intrinsic pathway through the catalytic cut of Bid protein [7, 8]. The consequence of the imbalance between the levels of anti-apoptotic and pro-apoptotic Bcl-2 proteins caused by the action of truncated Bid protein is the release of cytochrome c from the mitochondria and the activation of caspase-9 [6]. The intrinsic pathway can be directly activated by various apoptosis inducers, including chemotherapeutic drugs that target mitochondria, causing the release of cytochrome c, which is involved in apoptosome formation and the activation of caspase-9 [9-11]. The activation of the executioner caspases by caspase-8 and caspase-9 leads to the well-described morphological changes typical for apoptotic cells, including their disintegration into apoptotic bodies [12, 13].

The U937 cell line is commonly used as a cell model, including for studies of the mechanisms of cell death [14, 15]. It is also used for the assessment of tumor necrosis factor alpha (TNFα) [16], the evaluation of novel anticancer drugs [10, 11, 17] and as an *in vitro* test system to identify contact sensitizers [18].

Bigda et al. identified the variant cell line $U937_V$ and found that it exhibits a different pattern of response to TNFα when compared with the original U937 cell line [16]. We compared the cytotoxic effect of TNFα on the $U937_V$ and U937 lines and found that $U937_V$ cells were sensitive to TNFα in the presence

and absence of the protein-synthesis inhibitor cycloheximide (CHX), whereas U937 cells (derived as a standard reference cell line from the American Type Culture Collection) only showed sensitivity to TNFα in the presence of CHX.
In this paper, we report on the typical morphology of cell death in $U937_V$ cells. It is characterized by a lack of cell disintegration. We evaluated whether the process of defective cell death can be induced in $U937_V$ cells not only by TNFα, the extrinsic pathway activator, but also by etoposide (VP-16) [19, 20]. This chemotherapeutic inhibits the enzyme topoisomerase II, which unwinds DNA and by doing so causes DNA double-strand breaks [21]. In consequence, it can induce the intrinsic pathway of apoptosis. Next, we aimed to find out if the cell death in the two cell lines will show features characteristic of apoptosis when activated by either of the two apoptotic inducers. Additionally, we compared the dynamics of the molecular events that occurred during the cell death processes induced by TNFα and etoposide. Thus, we could establish that the atypical morphology of the dying cells may be a characteristic feature of the variant cell line rather than an effect that is only specific to the type of stimuli.

MATERIALS AND METHODS

Cells and media

The U937 cell line was derived from histiocytic lymphoma cells [22]. The variant cell line $U937_V$ was described previously [16]. Cells were cultured at 37ºC in a humidified atmosphere (5% CO_2) in complete medium (RPMI 1640 medium with 2 mM L-glutamine (Cytogen, Germany), supplemented with 10% fetal bovine serum (Cytogen, Germany), 1 mM sodium pyruvate, 100 U/ml penicillin and 100 μg/ml streptomycin. Both cell lines were free of mycoplasma.

Induction of cell death

Most of the analyses were performed after cell death was induced in the cell lines. In order to compare the biochemical changes in the dying process induced by the activation of the distinct apoptotic pathways, two cell death inducers were used. To induce the extrinsic pathway of apoptosis mediated by the death receptor pathway, the cells were exposed to 1000 U/ml TNFα (Beromun, Boehringer Ingelheim Limited, UK, 200 μg/ml) combined with 2 μg/ml CHX. To induce the intracellular pathway of apoptosis, the cells were exposed to 50 μg/ml VP-16 (Vepesid, Bristol-Myers Squibb S.p.A., Italy).

DNA fragmentation analysis

Seven million cells were seeded on 35-mm diameter culture plates with 4 ml of RPMI 1640 medium, and treated with the above-mentioned apoptotic inducers for 4 h at 37ºC. After stimulation, the cells were centrifuged (400 × g, 5 min, room temperature), the supernatant was discarded and the cellular pellet was resuspended in 4 ml of cold ethanol and stored for at least 24 h at -20ºC. Then the cells were centrifuged (800 × g, 5 min, 4ºC), 3 ml of ethanol were removed and the pellet was resuspended in 1 ml of the remaining ethanol. The cell

suspension was transferred to a 1.5-ml tube and centrifuged (800 × g, 5 min, 4ºC). Subsequently, the cell pellets were lysed in 100 µl of lysing buffer (10 mM Tris, 10 mM EDTA, 0.5% Triton X-100, pH 8.0). After 10 min incubation at 4ºC, the cell lysates were centrifuged (20000 × g, 30 min, 4ºC) and the supernatants were transferred to new tubes. RNase was added to a final concentration of 200 µg/ml and incubated at 37ºC for 60 min. Then, proteinase K was added to a final concentration of 200 µg/ml and incubated at 37ºC for 60 min. DNA precipitation was performed using 50% 2-propanol and 0.5 M NaCl for 24 h at -20ºC. The obtained precipitate was centrifuged (20000 × g, 30 min, 4ºC) and the supernatant was discarded. The precipitate was air dried and dissolved in 15 µl of TE buffer (10 mM Tris, 1 mM EDTA). Finally, 5 µl of loading buffer was added and the DNA was separated on a 1.8% agarose gel.

Flow cytometry analysis

Early apoptosis was evaluated by measuring the exposure of phosphatidylserine on the outer leaflet of the plasma membrane. The analysis was performed using FITC-conjugated annexin-V (Annexin V-FITC Apoptosis Kit, MBL International). One hundred thousand cells were washed in 200 µl PBS, centrifuged and then resuspended in 100 µl binding buffer. Then, the cells were incubated for 5 min at 37^{o}C with 2 µl of FITC-conjugated annexin-V and 5 µl of propidium iodide. Four subpopulations were identified according to their fluorescence: PI-low/FITC-low (live cells), PI-high/FITC-low (necrotic cells), PI-low/FITC-high (early apoptotic cells), and PI-high/FITC-high (late apoptotic cells).

Mitochondrial membrane potential (MMP) was evaluated using tetramethylrhodamine methyl ester (TMRM, Fluka). U937 cells were stained with 0.1 µM TMRM for 30 min at 37^{o}C before the end of treatment with apoptotic inducers. Afterwards, the cells were centrifuged and resuspended in 250 µl of fresh RPMI 1640 medium for analysis.

The analysis of the superoxide anion levels was performed with dihydroethidium (DHE, Fluka). Cells were stained with 10 µM DHE 30 min at 37^{o}C before the end of treatment with apoptotic inducers. After staining, the cells were centrifuged and resuspended in 250 µl of fresh RPMI 1640 medium for analysis. The cells with higher superoxide anion concentrations were characterized with higher fluorescence intensity.

Caspase-9 activity was measured using the Caspase-9 Detection Kit FITC-LEHD-FMK (Calbiochem) following the manufacturer's instructions. The fluorescent marker FITC-LEHD-FMK is a labeled, cell-permeable, non-toxic inhibitor that binds irreversibly to activated caspase-9 in living cells. The data analysis was based on the evaluation of the percentage of cells expressing activated caspase.

The analysis was performed using an LSR II (Becton Dickinson, USA) and a Cytomics FC 500 (Beckman Coulter, Inc., USA) both equipped with an air-cooled argon ion laser (488 nm and respectively 15 and 20 mW). These standard instruments have two light scatter detectors for measuring the forward scatter

(which gives an estimation of cell size) and the side scatter (which gives an estimation of intracellular granularity), and four photomultiplier tubes that detect the appropriately filtered light at 525 ± 20 nm (Annexin V-FITC, FITC-LEHD-FMK, DCF), 570 ± 26 nm (PI, TMRM) and 625 ± 20 nm (Ethidium). All the measurements were performed for 10,000 cells by gating the cells that exhibited the typical forward and side scatter features of non-disintegrated cells. Data were analyzed offline using the BD FACSDiva (BD Biosciences, USA) or CXP software (Beckman-Coulter, CA, USA).

Fluorescence microscopy analysis

Fluorescence microscopy was performed using an IN Cell Analyzer 1000 (GE Healthcare, USA) for time-lapse fluorescence microscopy and an Axiovert 200 (Zeiss, Germany) for standard fluorescence microscopy. A time-lapse experiment was performed to evaluate the morphological changes in the dying cells. Cells were seeded on 96-well plates (3×10^5/well) and incubated with 7 ng/ml BODIPY (boron-dipyrromethene, Molecular Probes) to stain the membrane lipids, 3 µg/ml Hoechst 33342 (Molecular Probes) to stain the living cell nuclei and 3 µg/ml propidium iodide (Sigma-Aldrich) to stain the nuclei of dead cells (30 min at 37°C). After staining, the cells were treated with an apoptosis inducer (TNFα/CHX) and photographs were taken at 10× every 10 min.

Cytochrome c release

One million each of U937 and $U937_V$ cells were treated with TNFα/CHX or VP-16 for 4 h. After the treatment, the cells were harvested and centrifuged (400 × g, 5 min, 4ºC). Then, the cells were washed twice with PBS × 1 and resuspended in 500 µl of lysis buffer (Hepes 20 mM, KCl 10 mM, EDTA 1.5 mM, $MgCl_2$ 1 mM, DTT 1 mM, sucrose 250 mM) [10]. The cell lysate was centrifuged (22000 × g, 15 min, 4ºC) and the supernatant was separated from the cell fragments, enabling the separation of the post-mitochondrial fraction. The post-mitochondrial fraction of proteins was analyzed using 4% (upper gel) and 12% (resolving gel) SDS-PAGE under reducing conditions. The gel was transferred to a PVDF membrane and the membrane was probed with a 1:300 dilution of primary antibodies (mouse anti-cytochrome c, BD Pharmingen, USA). Affinity-purified anti-mouse IgG (Santa Cruz Biotechnology, USA) conjugated with HRP (horseradish peroxidase 1:3000) was used as a secondary antibody. BM Chemiluminescence Blotting Substrate (Roche, Switzerland) was used to visualize the protein bands.

Statistical analysis

Statistical differences between the two variants of the U937 cell line were determined using the U Mann-Whitney test (Statistica 10), after checking the normal distribution of the data. The analyses were performed using 5 to 15 replicates run in at least three independent experiments.

RESULTS

Unique $U937_V$ cell death is induced by both extrinsic and intrinsic pathway stimulators

The reference and variant U937 cell lines showed similar morphological changes in the initial stage of cell death after treatment with either TNFα/CHX or VP-16, which respectively activate the extrinsic or intrinsic pathways of apoptosis. The U937 cells died showing the characteristic morphological features of apoptosis (blebbing, formation of apoptotic bodies and cell disintegration), whereas the $U937_V$ cells went through the blebbing process but did not disintegrate, and instead regained their round shape (Fig. 1A).

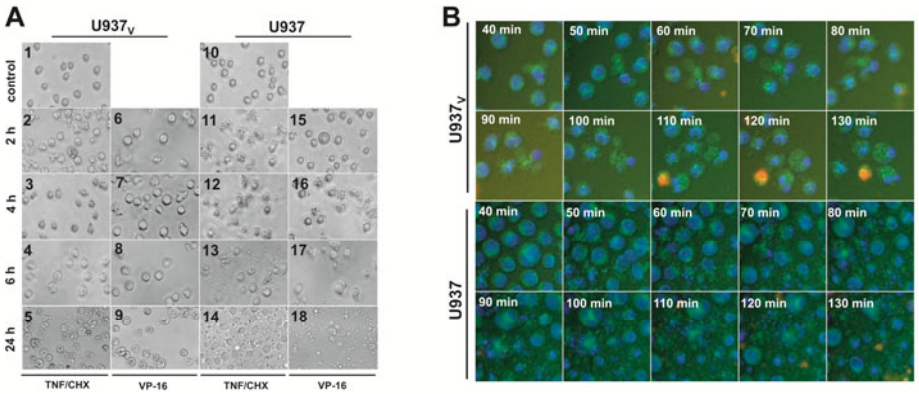

Fig. 1. The morphology of dying U937 cell line variants. A – Light microscopy photographs taken with a 10× objective of cells treated with TNFα (1000 U/ml) and CHX (2 μg/ml) or with VP-16 (50 μg/ml) for 6 h. 1 and 10 show control cells. In 2, 3, 6, 7, 11, 12 and 16 the blebbing process is visible. 3, 4, 5, 7, 8 and 9 show a lack of cell disintegration. In 13, 14, 17 and 18 there is disintegration of cells into apoptotic bodies. B – Time-lapse experiment. Cells treated with TNFα (1000 U/ml) and CHX (2 μg/ml) were stained with Hoechst 33342 (nuclei, in blue), BODIPY (boron-dipyrromethene, cell membranes, in green) and propidium iodide (necrotic cells, in red).

To investigate the morphological changes that occur during the process of $U937_V$ death in detail, we performed a time-lapse fluorescence microscopy assay. Cells were stained with BODIPY, Hoechst 33342 and propidium iodide and photographed with a 10× objective at 10-min time intervals. During the initial treatment time, the morphological changes in the U937 and $U937_V$ cells were similar: the process of blebbing was visible, followed by apoptotic body formation (Fig. 1B). From this point on, the morphological differences between the U937 cell line variants became obvious: there was no disintegration into apoptotic bodies in the $U937_V$ cells but rather a reversal of the apoptotic body or a fusion of neighboring cells (or cell-like structures). Furthermore, the vast majority of the cell-like structures formed from the dying $U937_V$ cells kept the integrity of their membranes and did not incorporate propidum iodide, as

observed during the time-lapse experiment. The 24-hour observations of $U937_V$ cells showed that the cells continued to maintain their shape and did not disintegrate (Fig. 1A).

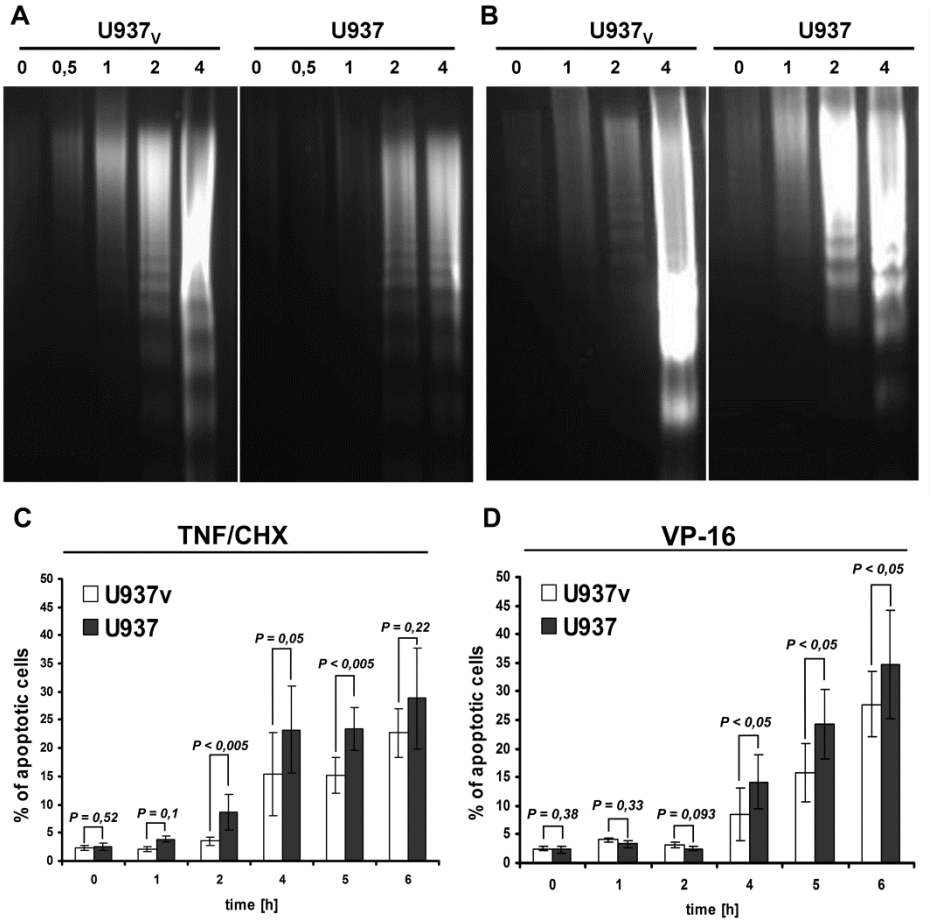

Fig. 2. Basic features of apoptosis. a and b. DNA fragmentation. U937 cell line variants were treated with apoptotic inducers for 0 to 4 h. A 1.8 % agarose gel electrophoresis with ethidium bromide was carried out with DNA isolated from the cells after each treatment. A – The DNA ladder was produced through treatment with TNFα (1000 U/ml)/CHX (2 μg/ml). B –The DNA ladder was produced through treatment with VP-16 (50 μg/ml). C and D – Phosphatidylserine exposure on the outer leaflet of the cell membrane. Percentage of apoptotic cells was obtained by flow cytometry using the Annexin V-FITC/PI Apoptosis Kit. Both variants of the U937 cell line were treated with TNFα (1000 U/ml)/CHX (2 μg/ml, A) or with VP-16 (50 μg/ml, B) for 0 to 6 h. The results show the mean number of cells with a positive FITC signal (in percentage) ± SD (n = 5). Negligible PI-positive cells were detected (result not shown).

Identification of apoptosis in the dying U937$_V$ cells stimulated by two types of apoptotic inducers

The morphological differences between the two cell lines could result from the induction of different cell death mechanisms. However, we showed that both cell types displayed the basic features of apoptotic cell death regardless of the pathway activated. Namely, in both cell lines treated with either cell death activator, oligonucleosomal fragmentation of DNA was observed, and no major differences were found between the kinetics of appearance of the DNA ladder. However, more extensive oligonucleosomal DNA fragmentation was found in U937v cells than in U937 cells after 4 h treatment (Fig. 2A and B).

The exposure of phosphatidylserine (PS) on the outer leaflet of the cell membrane was evaluated by flow cytometry as a critical parameter for the recognition and phagocytosis of apoptotic cells by engulfing cells. During this analysis, it was observed that treatment with either apoptosis inducer (TNFα/CHX, Fig. 2C; VP-16, Fig. 2D) resulted in PS exposure in both cell lines, although it was slightly more effective in the U937 cells. It is worth emphasizing that the number of cells with high PI fluorescence during 6 h of cell death induction was negligible and found to be lower in the U937$_V$ cells than in the reference cells (data not shown). Only after 24 h of induction of cell death was secondary necrosis observed in the two cell types (data not shown) [5].

Different kinetics of some other apoptotic events were also identified in U937$_V$ cells when compared with the reference cells. The analysis of caspase-9 activity revealed that its activity was consistently detectable in >50% of U937v cells after just 4 h of stimulation, while in the reference cells, this level of activation was only observed after 6 h (Fig. 3A and B).

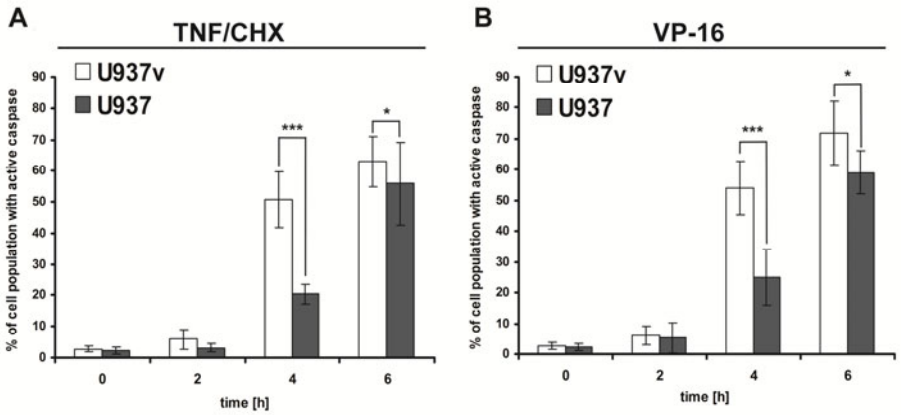

Fig. 3. Caspase-9 activation during apoptosis. A and B – Percentage of cells with caspase-9 activity. Both variants of the U937 cell line were treated with A – TNFα (1000 U/ml) and CHX (2 μg/ml) or B – VP-16 (50 μg/ml) for 0 to 6 h. The results show the mean of number of cells with a positive FITC-LEHD-FMK signal (in percentage) ± SD (n = 5). Statistically significant differences between the two cell line variants are indicated (***$p < 0.01$).

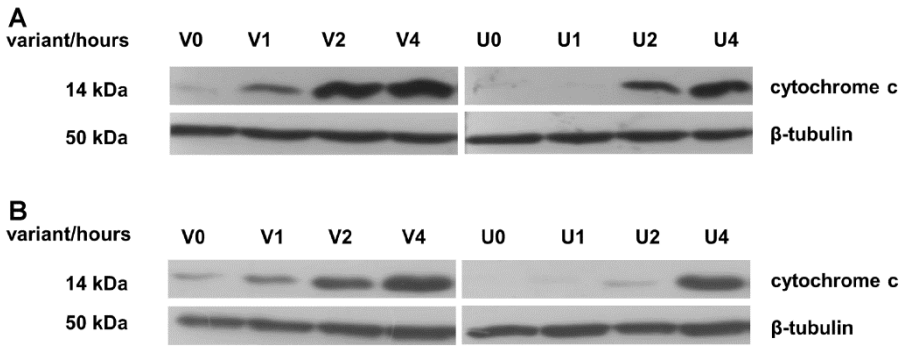

Fig. 4. Western Blot analysis of cytochrome c release. Both variants of the U937 cell line were treated with A – TNFα (1000 U/ml) and CHX (2 μg/ml), or B – VP-16 (50 μg/ml) for 0, 1, 2 or 4 h, then lysed. Their proteins were separated by PAGE. After transferring the proteins to a PVDE membrane, the intracellular cytochrome c present in the cytosolic fraction of the proteins was detected using monoclonal antibodies. β-tubulin was used as a protein quantity marker. Treatments of $U937_V$ are represented as V0-V4 (the numbers correspond to the length of stimulation) and U937 treatments are represented as U0-U4.

An analysis of cytochrome c release from the mitochondria was carried out to understand the phenomenon of early detection of strong caspase-9 activity in $U937_V$ cells undergoing apoptosis (Fig. 4). The results obtained showed that in $U937_V$ cells, the release of cytochrome c to the cytosol occurred earlier than in U937 cells. Cytochrome c was already present in the cytosol of U937v cells after 1 h of treatment with TNFα/CHX (Fig. 4A) or VP-16 (Fig. 4B). After 2 h of treatment with the cell death inducers, the presence of cytochrome c in the cytosolic extracts was more prominent in the variant cells.

A study of the mitochondria in dying $U937_V$ cells showed that the mitochondrial membrane potential (MMP) dropped rapidly after 2 h treatment with either of the cell death inducers. A decrease in MMP in U937 cells was also visible, but less pronounced and detected later at the later times of stimulation (Fig. 5A and B). Cells with lower MMP were characterized by lower fluorescence. The mitochondria are the major source of reactive oxygen species (ROS) in the cell, and these are also generated during apoptosis when the MMP is disturbed. In our study, the analysis of the superoxide anion ($^{\cdot}O_2^-$, Fig. 5C and D) showed a statistically significant increase in $U937_V$ cells, mostly after 6 h of treatment. No significant increase in $^{\cdot}O_2^-$ or ROS levels was noted in the reference cells.

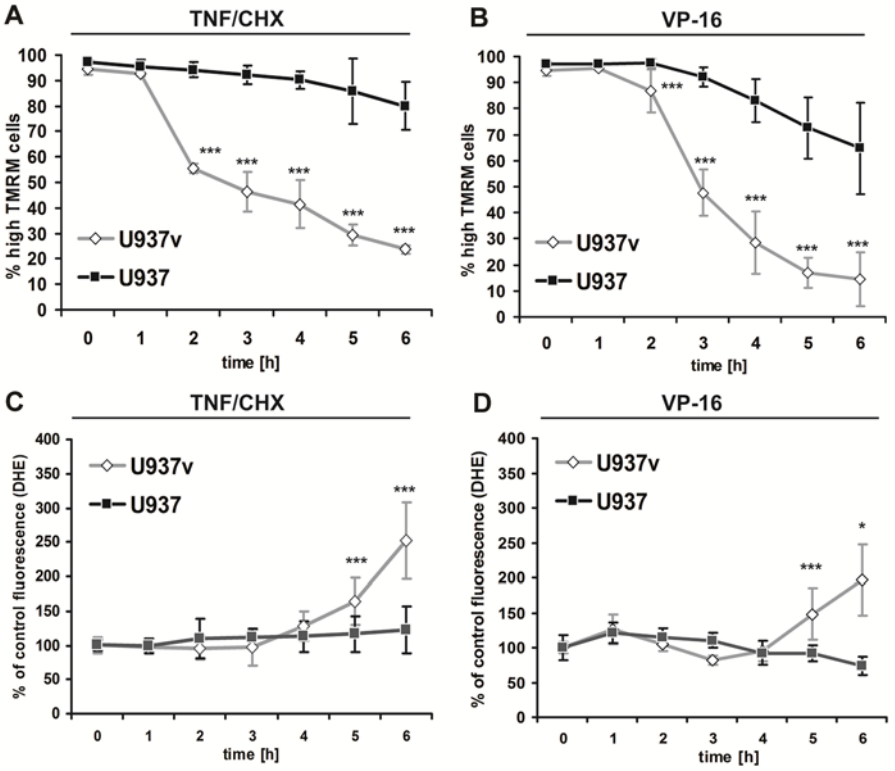

Fig. 5. Mitochondrial features of the dying process of U937 cell line variants. A and B – Mitochondrial membrane potential. Flow cytometric analysis of MMP with TMRM in cells treated with A – TNFα (1000 U/ml) and CHX (2 μg/ml), or B – VP-16 (50 μg/ml) for 6 h. The results represent the mean of number of cells with high MMP (high TMRM fluorescence) ± SD (n = 6). C and D – Superoxide anion level. Cells were treated with C – TNFα (1000 U/ml) and CHX 2 μg/ml), or D – VP-16 (50 μg/ml) for 6 h. DHE fluorescence indicates the level of superoxide anions. The 100% value is the average fluorescence of DHE for untreated cells. The results represent the mean ± SD (n = 7). Statistically significant differences between the two cell line variants are indicated (*$p < 0.05$; ***$p < 0.005$).

DISCUSSION

The two variants of the U937 cell line used in this study were previously characterized by their different susceptibility to TNFα in the absence of the protein synthesis inhibitor cycloheximide [16]. In this study, we applied two distinct inducers of apoptosis, namely TNFα in the presence of CHX, which activates the apoptotic process through the extrinsic signaling pathway, or etoposide, which activates it through the intrinsic signaling pathway. We observed an atypical death mode, characterized by a lack of cell disintegration. Furthermore, we verified that in the two cell lines either type of apoptotic inducer could activate the cell death process with the characteristic biochemical features of apoptosis.

The typical morphological and biochemical features of apoptotic cells are plasma membrane blebbing (zeiosis), the formation of apoptotic bodies, the preservation of cell membrane integrity during the early stages of the process, internucleosomal DNA degradation, and the exposure of phosphatidylserine on the outer leaflet of the cell membrane [2, 5, 23]. All of these features of apoptosis were observed during the dying process of the $U937_V$ cells. However, the lack of final cell disintegration suggested that a defective process of apoptosis was occurring. This atypical cell death mechanism was activated similarly by both inducers of apoptotic pathways. This also indicated that the apoptosis defect observed in the $U937_V$ cells concerned the later stages, which are shared by the different apoptotic signaling pathways.

Further analysis showed that some of the apoptotic events observed in $U937_V$ cells were accelerated and more pronounced than in dying U937 cells. A faster and more pronounced decline in mitochondrial membrane potential (MMP) and a faster release of cytochrome c could result in a more effective activation of caspases, which was observed in the $U937_V$ cells. These facts collectively suggested that the mitochondria of $U937_V$ cells are more sensitive to the induction of apoptosis than those of the reference cells. This could also result in possible disturbances in the generation of ATP, proper levels of which are critical for the execution of apoptosis [19, 24, 25]. Our preliminary studies indicate that both apoptotic stimuli induce a much deeper decrease in ATP levels in $U937_V$ cells when compared to the reference cells. Additionally, a rapid decrease in MMP might suggest that ATP is depleted and the process of apoptosis might be inhibited [24, 26]. Although an MMP decrease can be a consequence of the presence of reactive oxygen species (ROS) [8], in our study the generation of ROS observed in the $U937_V$ cells seemed to be rather the consequence of a decrease in the MMP, similarly to that reported by other authors [9, 27, 28].

The final consequence of the defective apoptosis of $U937_V$ cells is the lack of disintegration into apoptotic bodies. Physiologically, these “products” of apoptosis can be easily targeted by the phagocytic cells [25, 29]. The lack of cell disintegration can have serious repercussions, as the unusually dying cell remnants seem to have a significant impact on the immune system [30]. The clearance process should be rapid and precede the irreversible changes in apoptotic bodies that result in secondary necrosis [1, 23, 25]. Thus, the effective clearance of apoptotic bodies helps to avoid the inflammatory response or an uncontrolled release of potentially immunogenic cellular components [31, 32]. The size of the apoptotic cell remnants may principally influence the feasibility of their engulfment [25]. Therefore, the atypical mechanism of cell death may have a significant influence on the type and effectiveness of the immune response. Further studies on the immune consequences of an atypical mechanism of death of the variant of the U937 cell line would be useful from a clinical point of view.

We propose the $U937_V$ cell line as a model for future studies on mechanisms governing the process of cell disintegration into apoptotic bodies. Uncovering the underlying molecular mechanism of the apoptosis defect in $U937_V$ cells may

identify new possibilities for the modulation of apoptosis in other cells, especially affecting the final phase of apoptosis, when important interactions with components of the immune system appear. Moreover, the U937 reference and $U937_V$ variant cells described in this study can already be offered as a useful comparison model for basic studies of the apoptotic process, especially concerning the events leading to the formation of apoptotic bodies and to cell disintegration.

Acknowledgments. We would like to thank Laura Díaz Vico, Domingo Gil Casanova, Elżbieta Goyke, Guadalupe Herrera Martín, Carmen Navarro Rey and Alicia Martínez Romero for their excellent technical assistance, and Jolanta Grzenkowicz for her advice on methodology throughout this project. We would also like to acknowledge funding from the Leonardo da Vinci project scheme for cooperation with the Valencia lab (awarded to Grzegorz Stasiłojć), and from the core fund of the Intercollegiate Faculty of Biotechnology (2008-2010) and project No. N N401 196939 of the National Science Centre (2010-2012).

REFERENCES

1. Viorritto, I.C.B., Nikolov, N.P. and Siegel, R.M. Autoimmunity versus tolerance: can dying cells tip the balance? **Clin. Immunol.** 122 (2007) 125-134.
2. Gurumurthy, S., Vasudevan, K.M. and Rangnekar, V.M. Regulation of apoptosis in prostate cancer. **Cancer Metastasis Rev.** 20 (2001) 225-243.
3. Böhm, I. and Schild, H. Apoptosis: the complex scenario for a silent cell death. **Mol. Imaging Biol.** 5 (2003) 2-14.
4. Bras, M., Queenan, B. and Susin, S.A. Programmed cell death via mitochondria: different modes of dying. **Biochemistry (Mosc)** 70 (2005) 231-239.
5. Krysko, D.V., VandenBerghe, T., D'Herde, K. and Vandenabeele, P. Apoptosis and necrosis: detection, discrimination and phagocytosis. **Methods** 44 (2008) 205-221.
6. Oliveira, J.B. and Gupta, S. Disorders of apoptosis: mechanisms for autoimmunity in primary immunodeficiency diseases. **J. Clin. Immunol.** 28 Suppl. 1, (2008) S20-8.
7. Jana, N.R. NSAIDs and apoptosis. **Cell Mol. Life Sci.** 65 (2008) 1295-1301.
8. Festjens, N., VandenBerghe, T. and Vandenabeele, P. Necrosis, a well-orchestrated form of cell demise: signalling cascades, important mediators and concomitant immune response. **Biochim. Biophys. Acta** 1757 (2006) 1371-1387.
9. Groninger, E., Meeuwsen-De Boer, G.J., De Graaf, S.S.N., Kamps, W.A. and De Bont, E.S.J.M. Vincristine induced apoptosis in acute lymphoblastic leukaemia cells: a mitochondrial controlled pathway regulated by reactive oxygen species? **Int. J. Oncol.** 21 (2002) 1339-1345.
10. Liao, P. and Lieu, C. Cell cycle specific induction of apoptosis and necrosis by paclitaxel in the leukemic U937 cells. **Life Sci.** 76 (2005) 1623-1639.

11. Cerella, C., Scherer, C., Cristofanon, S., Henry, E., Anwar, A., Busch, C., Montenarh, M., Dicato, M., Jacob, C. and Diederich, M. Cell cycle arrest in early mitosis and induction of caspase-dependent apoptosis in U937 cells by diallyltetrasulfide (Al2S4). **Apoptosis** 14 (2009) 641-654.
12. Van Hoof, C. and Goris, J. Phosphatases in apoptosis: to be or not to be, PP2A is in the heart of the question. **Biochim. Biophys. Acta** 1640 (2003) 97-104.
13. Hail, N.J. Mitochondria: A novel target for the chemoprevention of cancer. **Apoptosis** 10 (2005) 687-705.
14. Hori, T., Kondo, T., Tabuchi, Y., Takasaki, I., Zhao, Q., Kanamori, M., Yasuda, T. and Kimura, T. Molecular mechanism of apoptosis and gene expressions in human lymphoma U937 cells treated with anisomycin. **Chem. Biol. Interact.** 172 (2008) 125-140.
15. Ho, S., Chen, W., Chiu, H., Lai, C., Guo, H. and Wang, Y. Combination treatment with arsenic trioxide and irradiation enhances apoptotic effects in U937 cells through increased mitotic arrest and ROS generation. **Chem. Biol. Interact.** 179 (2009) 304-313.
16. Kaszubowska, L., Engelmann, H., Gotartowska, M., Iliszko, M. and Bigda, J. Identification of two U937 cell sublines exhibiting different patterns of response to tumour necrosis factor. **Cytokine** 13 (2001) 365-370.
17. Shin, D.Y., Kim, G.Y., Li, W., Choi, B.T., Kim, N.D., Kang, H.S. and Choi, Y.H. Implication of intracellular ROS formation, caspase-3 activation and Egr-1 induction in platycodon D-induced apoptosis of U937 human leukemia cells. **Biomed. Pharmacother.** 63 (2009) 86-94.
18. Python, F., Goebel, C. and Aeby, P. Assessment of the U937 cell line for the detection of contact allergens. **Toxicol. Appl. Pharmacol.** 220 (2007) 113-124.
19. Denecker, G., Vercammen, D., Declercq, W. and Vandenabeele, P. Apoptotic and necrotic cell death induced by death domain receptors. **Cell Mol. Life Sci.** 58 (2001) 356-370.
20. Takahashi, A., Masuda, A., Sun, M., Centonze, V.E. and Herman, B. Oxidative stress-induced apoptosis is associated with alterations in mitochondrial caspase activity and Bcl-2-dependent alterations in mitochondrial pH (pHm). **Brain Res. Bull.** 62 (2004) 497-504.
21. Smart, D.J., Halicka, H.D., Schmuck, G., Traganos, F., Darzynkiewicz, Z. and Williams, G.M. Assessment of DNA double-strand breaks and gammaH2AX induced by the topoisomerase II poisons etoposide and mitoxantrone. **Mutat. Res.** 641 (2008) 43-47.
22. Sundstrom, C. and Nilsson, K. Establishment and characterization of a human histiocytic lymphoma cell line (U-937). **Int. J. Cancer** 17 (1976) 565-577.
23. Ndozangue-Touriguine, O., Hamelin, J. and Bréard, J. Cytoskeleton and apoptosis. **Biochem. Pharmacol.** 76 (2008) 11-18.
24. Izyumov, D.S., Avetisyan, A.V., Pletjushkina, O.Y., Sakharov, D.V., Wirtz, K.W., Chernyak, B.V. and Skulachev, V.P. "Wages of fear": transient

threefold decrease in intracellular ATP level imposes apoptosis. **Biochim. Biophys. Acta** 1658 (2004) 141-147.
25. Orlando, K.A., Stone, N.L. and Pittman, R.N. Rho kinase regulates fragmentation and phagocytosis of apoptotic cells. **Exp. Cell Res.** 312 (2006) 5-15.
26. Salvioli, S., Barbi, C., Dobrucki, J., Moretti, L., Pinti, M., Pedrazzi, J., Pazienza, T.L., Bobyleva, V., Franceschi, C. and Cossarizza, A. Opposite role of changes in mitochondrial membrane potential in different apoptotic processes. **FEBS Lett.** 469 (2000) 186-190.
27. Chung, Y.M., Bae, Y.S. and Lee, S.Y. Molecular ordering of ROS production, mitochondrial changes, and caspase activation during sodium salicylate-induced apoptosis. **Free Radic. Biol. Med.** 34 (2003) 434-442.
28. Watabe, M. and Nakaki, T. ATP depletion does not account for apoptosis induced by inhibition of mitochondrial electron transport chain in human dopaminergic cells. **Neuropharmacology** 52 (2007) 536-541.
29. Krysko, D.V., D'Herde, K. and Vandenabeele, P. Clearance of apoptotic and necrotic cells and its immunological consequences. **Apoptosis** 11 (2006) 1709-1726.
30. Raina, A.K., Hochman, A., Zhu, X., Rottkamp, C.A., Nunomura, A., Siedlak, S.L., Boux, H., Castellani, R.J., Perry, G. and Smith, M.A. Abortive apoptosis in Alzheimer's disease. **Acta Neuropathol.** 101 (2001) 305-310.
31. Schrijvers, D.M., Martinet, W., De Meyer, G.R.Y., Andries, L., Herman, A.G. and Kockx, M.M. Flow cytometric evaluation of a model for phagocytosis of cells undergoing apoptosis. **J. Immunol. Methods** 287 (2004) 101-108.
32. Petrovski, G., Zahuczky, G., Katona, K., Vereb, G., Martinet, W., Nemes, Z., Bursch, W. and Fésüs, L. Clearance of dying autophagic cells of different origin by professional and non-professional phagocytes. **Cell Death Differ.** 14 (2007) 1117-1128.